SOILS AND FOUNDATIONS Vol. 38, No. 3, 129-142, Sept. 1998
Japanese Geotechnical Society

NON-LINEAR SOIL PROPERTIES AND IMPEDANCES FOR AXIALLY VIBRATING PILE ELEMENTS

OD. MICHAELIDES[i], G. BOUCKOVALAS[ii] and G. GAZETAS[iii]

ABSTRACT

Dynamic soil properties around axially vibrating piles are generally non-uniform even in homogeneous soils. This is a result of the non-linear soil reaction to the radially decreasing stresses and strains induced by the pile, as well as the slippage at the pile-soil interface. To improve the accuracy of analytical computations, this paper focusses upon the nonlinear soil response anticipated in the field and establishes the radial variation of soil properties based on commonly reported experimental data. In addition, solutions are presented for the corresponding impedance of the springs and dashpots used to represent soil in a Winkler-type analysis of axially vibrating piles. Slippage at the pile soil interface is taken into account assuming a rigid-perfectly plastic contact between the pile and the soil. To assess the relative effects of soil nonlinearity in practical applications, analytical results for different pile, load and soil conditions are presented in the form of diagrams and simple approximate relationships.

Key words: axial vibration, dynamic soil impedance, piles, soil nonlinearity (**IGC**: E8)

INTRODUCTION

Analysis of the dynamic axial response of piles is commonly based on the Winkler approach, initially conceived and used with success to simulate the response of statically loaded piles. Namely, the soil surrounding the pile is replaced by a series of independent springs and dashpots with frequency dependent characteristics (e.g. Novak 1974 and 1977). The basic assumption underlying this approach is that the vibrating pile generates exclusively shear waves (SV) propagating radially outwards in the horizontal plane. Thus, radial soil displacements are neglected and the soil is considered to deform axisymmetrically, in pure shear.

The frequency dependent moduli of the Winkler springs and dashpots, corresponding to the dynamic soil impedance, are obtained from the solution of the simplified elastodynamic problem of a unit thickness rigid and massless cylindrical pile element oscillating within a horizontal soil layer of infinite lateral extend. For the sake of simplicity, most available solutions assume that dynamic soil properties are radially uniform, although this is not true even for piles embedded into homogeneous soil deposits. In fact, the dynamic soil stiffness is lower and the hysteretic damping ratio is higher in the vicinity of the pile as compared to the far field. This is a result of the non-linear soil reaction to the radially decreasing stress and strain amplitudes induced by the vibrating pile, as well as of the slippage that may develop between the pile and the soil.

The first relevant solutions to this problem were presented by Novak and Sheta (1980), for the case of reduced shear modulus and increased hysteretic damping in a massless, narrow, annular boundary zone around the pile. The mass of the boundary zone was neglected on purpose in order to prevent fictitious wave reflections from the interface between the inner boundary zone and the free field. A later analysis of the same problem by Veletsos and Dotson (1986) included the inertia of the boundary zone. The solutions obtained in this way fluctuate with frequency due to the fictitious reflections, but reveal clearly that the inertia in the boundary zone has a quite substantial effect and should not be neglected. In order to eliminate the undesirable effects of internal wave reflection, the discontinuous variation of shear modulus with radial distance was later replaced by continuous, monotonically increasing variations (Gazetas and Dobry, 1984; Veletsos and Dotson, 1988; Dotson and Veletsos, 1990).

All previous solutions outline the potential effects of radial soil heterogeneity, but only in qualitative terms. This is because the assumed variations of soil properties

[i] Graduate Student, Geotechnical Division, National Technical University, Patission 42, Athens 106 82 Greece.
[ii] Associate Professor, ditto.
[iii] Professor, ditto.
Manuscript was received for review on June 24, 1996.
Written discussions on this paper should be submitted before April 1, 1999 to the Japanese Geotechnical Society, Sugayama Bldg. 4F, Kanda Awaji-cho 2-23, Chiyoda-ku, Tokyo 101-0063, Japan. Upon request the closing date may be extended one month.

are merely hypothetical and cannot be related to actual loading, pile and soil conditions encountered in practice. To overcome this shortcoming, one should first compute the radial distribution of stresses and strains in the soil around the pile, consequently determine the compatible shear modulus and hysteretic damping ratio, and finally solve the problem of dynamic pile-soil interaction.

The general feasibility of this approach has been recently demonstrated by Michaelides et al. (1997). Along the same lines, this paper proceeds with a refined simulation of the non-linear soil response and derives the corresponding variation of dynamic soil properties, as well as the moduli of the Winkler springs and dashpots. Implementation of the results presented herein to the computation of the dynamic axial response of piles is briefly discussed in Appendix I.

BASIC TERMS AND METHODOLOGY

Effect of Soil Nonlinearity

Figure 1 defines the basic terms used in the presentation and illustrates the mechanisms leading to radial heterogeneity around axially vibrating piles embedded in a layered soil. During application of static loading P_{st} on the pile head, shear stresses τ_{st} develop on vertical and horizontal planes which decrease with radial distance r from the pile axis. Once a harmonic load $Pe^{i\omega t}$ is added, dynamic shear stresses $\tau e^{i\omega t}$ are superimposed to the static ones, which also decrease in amplitude with radial distance away from the pile axis. Due to soil nonlinearity, the associated secant shear modulus G and the hysteretic damping ratio ξ are functions of the applied shear stresses and strains, and consequently they vary radially even if the initial soil properties are homogeneous.

To determine the distribution of G and ξ for actual pile, soil and loading conditions, it is first necessary to establish simple approximate relationships for the radial variation of the dynamic shear stress amplitudes around cylindrical pile elements. The corresponding values of shear modulus and hysteretic damping ratio are consequently determined based on two different sets of standardised experimental results from resonant column tests, for soils of different plasticity. Finally, the dynamic impedance of the soil around an axially vibrating pile segment is computed analytically by solving the elasto-dynamic equilibrium problem for the radial distribution of soil properties established previously. Soil impedance is expressed in complex form, as:

$$I_z = K_z + i\omega C_z \tag{1}$$

where the stiffness parameters K_z and C_z correspond to the moduli of the equivalent Winkler springs and dashpots respectively.

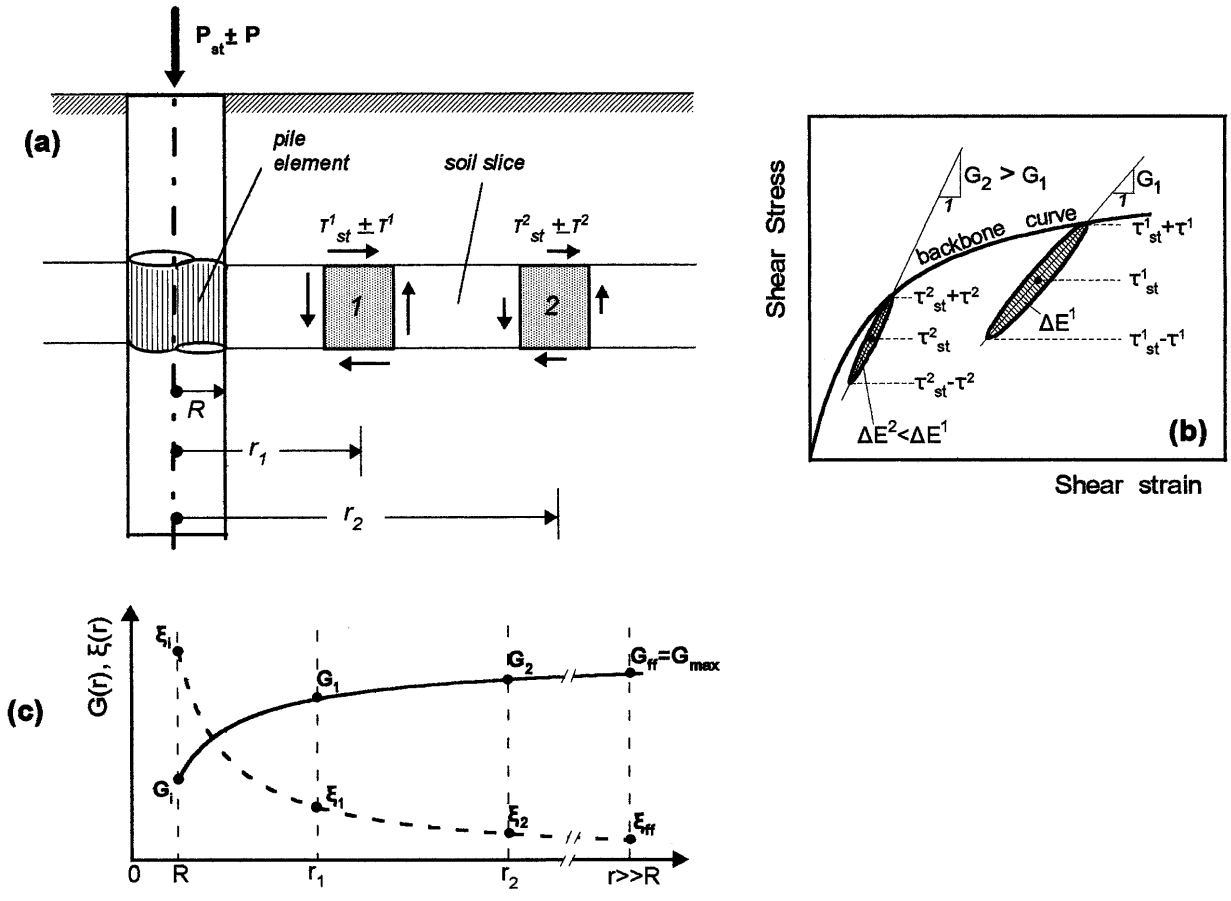

Fig. 1. Non-linear soil effects on dynamic soil properties: (a) Static and dynamic shear stresses in the soil; (b) Non-linear dynamic response of soil elements; (c) Radial variation of shear modulus and hysteretic damping ratio

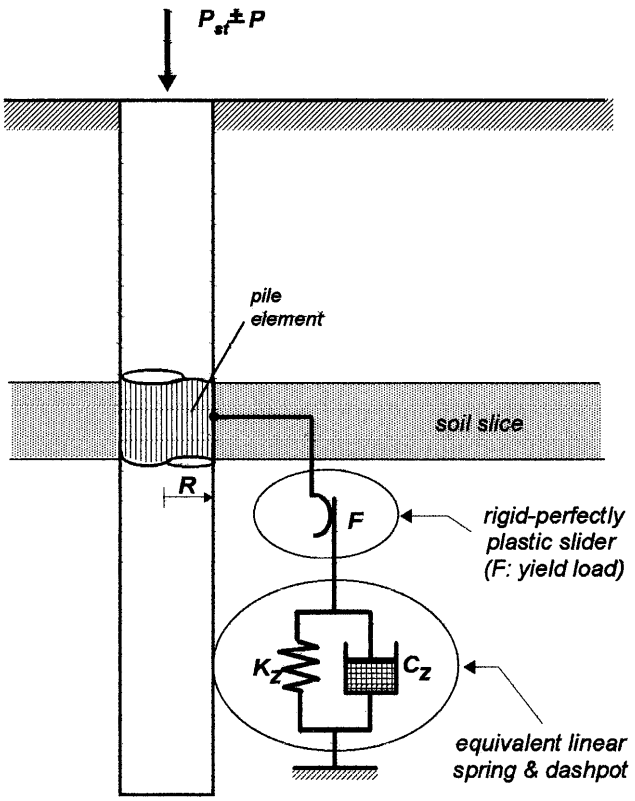

Fig. 2. Winkler representation of dynamic soil impedance and slippage at the pile-soil interface via an equivalent-linear spring and dashpot coupled to a rigid-perfectly-plastic slider

Effect of Slippage at the Pile-Soil Interface

In the previous outline it has been assumed that the pile element remains in firm contact with the soil throughout dynamic loading. Actually, slippage will occur whenever the sum of static and dynamic shear stresses applied at the pile-soil interface exceeds the unit skin friction f. Rigorous evaluation of this effect on the nonlinear dynamic stiffness of the pile element requires detailed modelling of the cyclic response of the interface and numerical implementation. However, to maintain the simplicity sought in this article, the relative effect of slippage is established based on the approximate model of Fig. 2: the soil is replaced by an equivalent linear spring-and-dashpot system with dynamic impedance I_z and the pile-soil interface is replaced by a rigid-plastic slider of yield load $F=\pi Df$ where D is the pile diameter. This is equivalent to an assumption that unloading-reloading of the pile-soil interface follows the Masing criteria for cyclic loading (Masing, 1926).

RADIAL VARIATION OF STATIC AND DYNAMIC SHEAR STRESSES

Static Shear Stresses

The static shear stresses in the soil surrounding an axially loaded pile element are expressed as (Baguelin and Frank, 1979; Randolph and Wroth, 1978):

$$\tau_{st}=\tau_{st,i}(R/r) \tag{2}$$

where $\tau_{st,i}=\tau_{st}(R)$ is the shear stress at the pile-soil interface and R is the pile radius. With very good proximity, Eq. (2) is valid for homogeneous as well as for laterally heterogeneous soils and suggests that the radial distribution of static shear stresses is not sensitive to the corresponding variation of soil properties.

Dynamic Shear Stresses in Homogeneous Soil

To compute the dynamic shear stresses, it is assumed that an axially vibrating cylindrical pile element generates only shear waves (SV) which propagate laterally under axisymmetric conditions. In that case, the equilibrium of shear and inertia forces acting on an elementary soil ring around the pile leads to the following differential equation of motion:

$$G(d^2W/dr^2)+(dG/dr+G/r)dW/dr=\rho d^2W/dt^2 \tag{3}$$

where $W=W(r)$ is the vertical displacement, ρ is the mass density and $G=G(r)$ is the shear modulus of the soil. For harmonic excitation with circular frequency ω (rad/s), and a homogeneous soil with constant hysteretic damping ratio $\xi(r)=\xi_i$ and shear modulus $G(r)=G_i$, the solution of Eq. (3) takes the form (e.g. Morse and Ingard, 1968):

$$W=A[J_0(\alpha)+iY_0(\alpha)]e^{-i\omega t} \tag{4}$$

where $\alpha=\omega r/V_i$ is a non-dimensional frequency parameter, $V_i=(G_i/\rho)^{1/2}$ is the shear wave velocity of the soil, J_0 and Y_0 are zero order Bessel functions of first and second kind respectively, and A is a constant of integration.

The dynamic shear stress amplitude τ corresponding to the displacement W is:

$$\tau=G_i|dW/dr|$$

or

$$\tau=-G_i(A\omega/V_i)[J_1^2(\alpha)+Y_1^2(\alpha)]^{1/2} \tag{5}$$

where J_1 and Y_1 are first order Bessel functions of the first and second kind respectively. Alternatively, in order to maintain the form of the respective relationship for the static shear stresses, Eq. (5) is written as:

$$\tau=\tau_i(R/r)F(\alpha) \tag{6}$$

where $\tau_i=\tau(R)$ is the dynamic shear stress amplitude at the pile-soil interface and

$$F(\alpha)=(\alpha/\alpha_i)[J_1^2(\alpha)+Y_1^2(\alpha)]^{1/2}/[J_1^2(\alpha_i)+Y_1^2(\alpha_i)]^{1/2} \tag{7}$$

with $\alpha_i=\omega R/V_i$.

Figure 3 shows the variation of the frequency dependent parameter $F(\alpha)$ for different values of α_i. It is observed that, for the values of α_i of practical interest (i.e. $\alpha_i<1.0$), $F(\alpha)$ may be computed from the much simpler expression:

$$F(\alpha)=\begin{cases}1.0 & \text{for } \alpha<1.0\\ \alpha^{0.50} & \text{for } \alpha\geq 1.0.\end{cases} \tag{8}$$

Equation (8) suggests that, $F(\alpha)$ increases monotonically

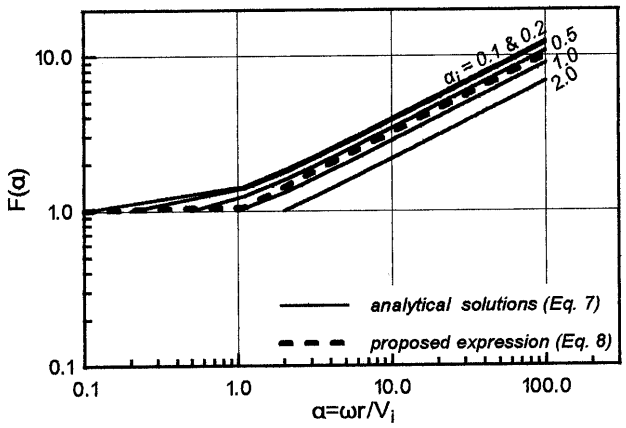

Fig. 3. Effect of non-dimensional frequency parameter α on the radial variation of dynamic shear stress amplitude

above unity as the non-dimensional radial frequency parameter α becomes gradually higher. In turn, this implies that the attenuation of dynamic shear stress amplitude is slower than that of static stresses, the difference increasing with the frequency of dynamic loading.

Dynamic Shear Stresses in Heterogeneous Soil

Equations (6) and (8) have been derived for the ideal case of an initially uniform distribution of shear modulus and hysteretic damping ratio in the soil. However, they can also be applied to compute the radial variation of soil properties in the case of non-uniform distributions of initial shear modulus and damping assuming that, as for static stresses, dynamic stress amplitudes are not sensitive to the exact variation of soil properties.

This assumption is evaluated in Fig. 4, where the solutions obtained for the radial distribution of dynamic shear stress amplitudes in homogeneous soils are compared to two alternative solutions for laterally heterogeneous soils with initial shear modulus and hysteretic damping ratio expressed in complex form as:

$$G^*=G_i\{1+i(2\xi_i)\}(r/R)^m \tag{9}$$

with $m=2/3$ and $m=1$. The detailed expressions for the radial distribution of dynamic stresses in these cases are summarised by Michaelides et al. (1997). The overall agreement between the solutions for homogeneous and heterogeneous soils is remarkably good, especially if one considers the extremely different distributions of shear modulus and hysteretic damping ratio assigned to the soil.

RADIAL VARIATION OF SHEAR MODULUS

In principle, the dynamic stress-strain response of the soil depends upon the static as well as the dynamic shear stress amplitudes. However, for moderate and low intensities of dynamic loading, one may overlook the effect of static shear stresses and focus upon the effect of dynamic shear stress or strain amplitudes. This approach is suggested by the well known Masing criteria (Masing, 1926) for unloading-reloading of soils and it is also substantiated by broad experimental evidence (e.g. Seed and Idriss, 1970; Iwasaki et al., 1978; Ishihara, 1982; Andersen et al.; 1988, Sagaseta et al., 1991). In fact, when the dynamic shear strain amplitude γ in the soil is lower than 10^{-3} or 10^{-2}, it is customary to describe the degradation of shear modulus by nonlinear relationships in terms of γ.

Figure 5 presents the experimental curves proposed by Vucetic and Dobry (1991) to describe the degradation of shear modulus ratio G/G_{max} with γ, where G_{max} denotes the shear modulus of the soil at very small shear strain amplitudes ($\gamma<10^{-5}$). According to these curves, the main factor which controls the G/G_{max}-γ relationship is soil plasticity, expressed via the plasticity index lp. Namely, for the same dynamic shear strain amplitude, the

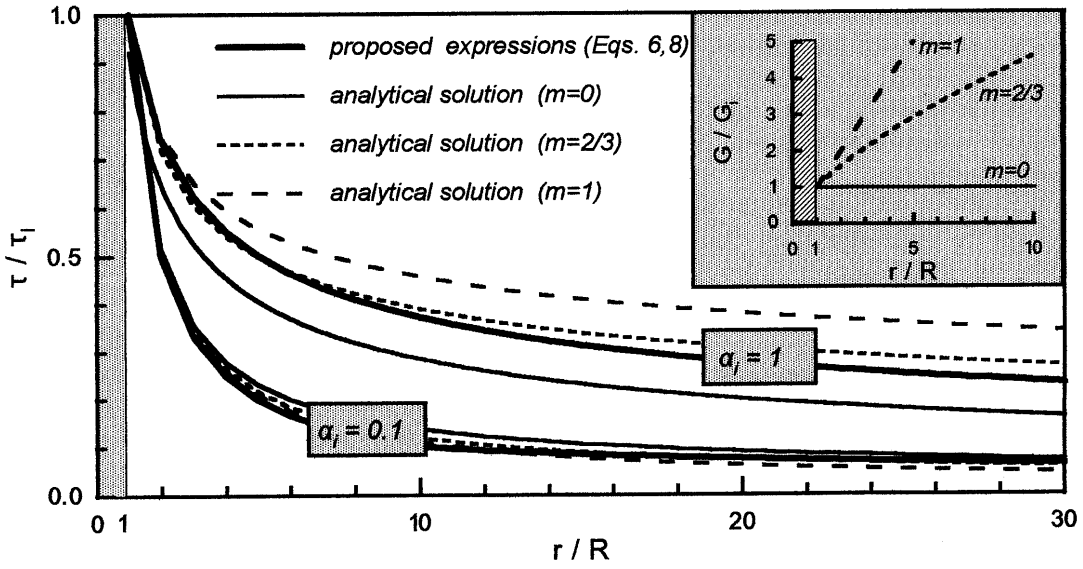

Fig. 4. Comparison of simplified relationships for the radial variation of dynamic shear stress amplitude to analytical solutions for homogeneous ($m=0$), as well as for heterogeneous soil ($m=2/3$ and 1)

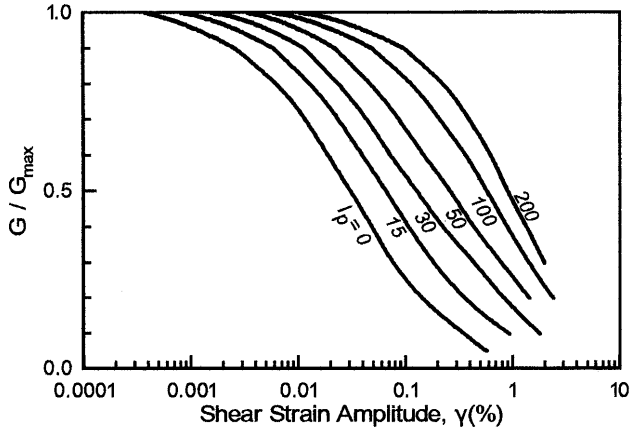

Fig. 5. Experimental curves for the non-linear variation of dynamic shear modulus versus shear strain amplitude proposed by Vucetic and Dobry (1991)

shear modulus degrades less as the value of lp increases.

More recently, Ishibashi and Zhang (1993) proposed the following empirical relationships to predict the reduction of shear modulus with dynamic shear strain amplitude:

$$G/G_{\max}=0.5\left\{1+\tan h\left[0.492\ln\frac{0.000102+n}{\gamma}\right]\right\}\sigma_0'^{m} \quad (10)$$

with

$$m=0.272\left\{1-\tan h\left[0.4\ln\frac{0.000556}{\gamma}\right]\right\}\times\exp\left(-0.0145lp^{1.3}\right) \quad (11)$$

and

$$n=\begin{cases}0.0 & \text{for } lp=0\\ 3.37\times10^{-6}lp^{1.404} & \text{for } 0<lp\le15\\ 7.0\times10^{-7}lp^{1.976} & \text{for } 15<lp\le70\\ 2.7\times10^{-5}lp^{1.115} & \text{for } lp>70.\end{cases} \quad (12)$$

This relationship is qualitatively similar to the experimental curves of Fig. 5, with only one difference: the effect of soil plasticity is now combined with the effect of effective confining pressure σ_0'. However, the additional effect of σ_0' is limited to non-plastic or low-plasticity soils and can be effectively overlooked for high plasticity soils with $lp>50\%$.

For the purposes of this study, the non-linear variation of shear modulus is expressed by the following general form:

$$G/G_{\max}=1-(B\gamma G/G_{\max})^{0.72}\exp(-lp/\lambda) \quad (14)$$

where lp is entered in percent (%), and the coefficients B and λ are determined from fitting Eq. (14) to the available experimental data. For instance, the following values were used to obtain an average fit of the experimental curves by Vucetic and Dobry (1991) and the analytical expressions by Ishibashi and Zhang (1993):

$$B=\begin{cases}2200 & \text{for Vucetic and Dobry (1991)}\\ 600 & \text{for Ishibashi and Zhang (1993)}\\ & \text{(average for } \sigma_0'=50\div400 \text{ kPa)}\end{cases} \quad (15)$$

and

$$\lambda=\begin{cases}21.5+0.25lp & \text{for Vucetic and Dobry (1991)}\\ 125 & \text{for Ishibashi and Zhang (1993)}\\ & \text{(independent from } \sigma_0').\end{cases} \quad (16)$$

Typical predictions of shear modulus degradation based upon Eq. (14) are compared to the experimental curves of Vucetic and Dobry (1991) and the relationships of Ishibashi and Zhang (1993) in Fig. 6.

To determine the radial variation of shear modulus, Eq. (14) is re-written in terms of the dynamic shear stress amplitude τ:

$$G/G_{\max}=1-(B\tau/G_{\max})^{0.72}\exp(-lp/\lambda). \quad (17)$$

Then, introducing Eq. (6) for the radial distribution of τ, the variation of shear modulus with radial distance is expressed as:

$$G/G_{\max}=1-\{\Lambda(R/r)F(\alpha)\}^{0.72} \quad (18)$$

where

$$\Lambda=B(\tau_i/G_{\max})\exp[-1.39(lp/\lambda)]. \quad (19)$$

Since the dynamic shear stress amplitude at the pile-soil interface τ_i is a fraction of the ultimate skin friction f, the cyclic loading intensity factor Λ is also written as:

$$\Lambda=B\mu(f/G_{\max})\exp[-1.39(lp/\lambda)] \quad (20)$$

where

$$\mu=\tau_i/f \quad (\le1.0). \quad (21)$$

At the pile soil interface ($r=R$), Eq. (18) yields:

$$G_i/G_{\max}=1-\{\Lambda F(\alpha_i)\}^{0.72} \quad (>0). \quad (22)$$

Taking into account that for usual soil and loading conditions $\alpha_i<1.0$ and consequently $F(\alpha_i)=1.0$, Eq. (22) implies that Λ ranges between 0.0 and 1.0.

Figure 7 shows the radial variation of shear modulus ratio $G/G_{\max}$ for different combinations of the loading intensity parameter Λ and the frequency parameter α_i. It is observed that:

(a) The radial variation of shear modulus is most rapid in the immediate vicinity of the pile, within a distance of two to four pile radii. At larger distances, the rate of change is substantially reduced and the shear modulus tends asymptotically to the corresponding free field value ($G\to G_{\max}$).

(b) The overall degradation of shear modulus increases as the loading intensity and frequency increase.

(c) At the pile-soil interface, the shear modulus ratio $G_i/G_{\max}$ is a unique function of Λ, i.e. it is independent of the loading frequency parameter α_i. This observation is also substantiated by Eq. (22).

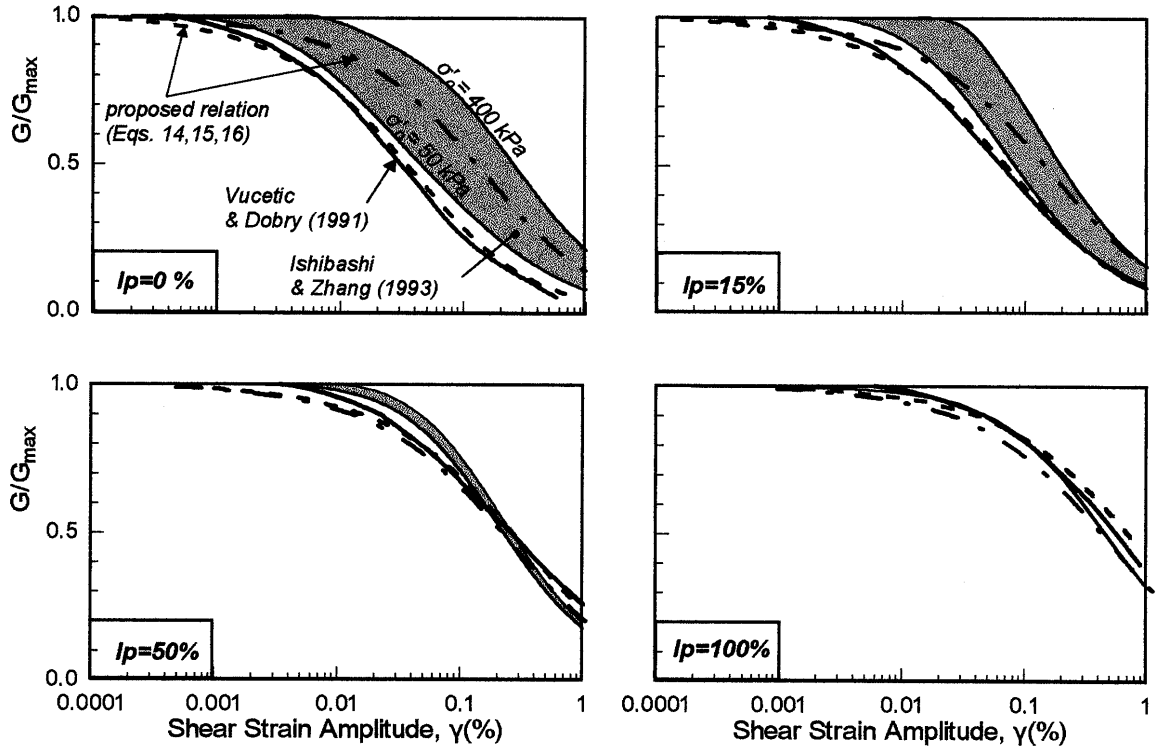

Fig. 6. Comparison of proposed G/G_{max}-γ relationship to empirical relationships proposed by Vucetic and Dobry (1991) and Ishibashi and Zhang (1993)

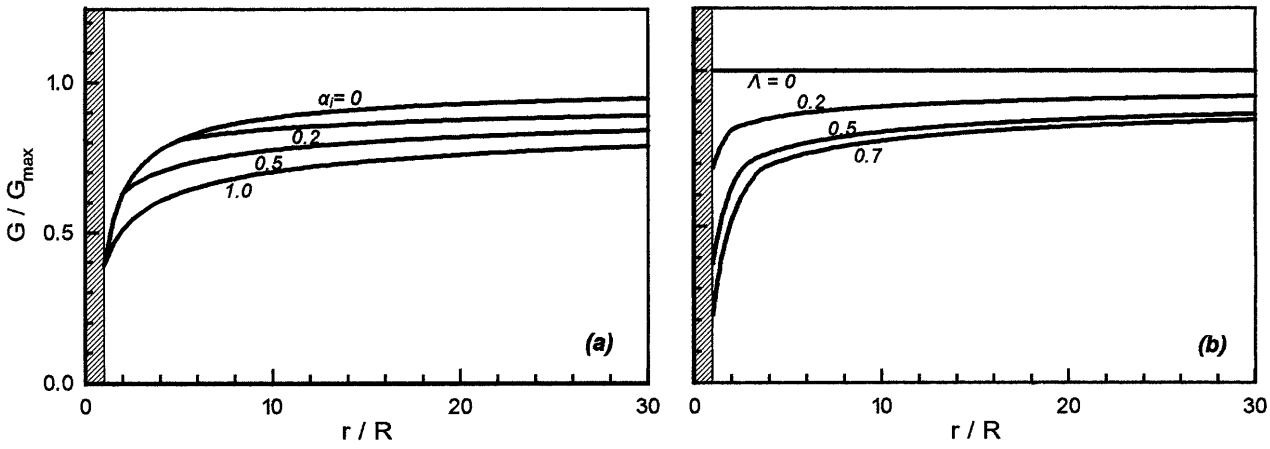

Fig. 7. Radial variation of dynamic shear modulus: (a) Effect of loading frequency a_i; (b) Effect of loading intensity Λ

RADIAL VARIATION OF HYSTERETIC DAMPING RATIO

The experimental curves proposed by Vucetic and Dobry (1991) to describe the variation of hysteretic damping ratio ξ with dynamic shear strain amplitude γ, for soils of different plasticity, are shown in Fig. 8(a). In contrast to the shear modulus behavior, the value of ξ corresponding to a given level of γ decreases as the soil becomes more plastic. The corresponding relationship between ξ and G/G_{max} is shown in Fig. 8(b). It is observed that ξ decreases as G/G_{max} increases, in a smooth nearly linear manner. Soil plasticity appears to affect the ξ-G/G_{max} relationship, but much less than the ξ-γ relationship in Fig. 8(a).

The corresponding analytical expressions of Ishibashi and Zhang (1993) draw upon the observation that the variation of ξ is influenced by the same factors as that of G/G_{max}. Hence, using Eq. (10) to compute the shear modulus ratio, the damping ratio is expressed as:

$$\xi = \frac{1+\exp(-0.0145 lp^{1.3})}{6} \times [0.586(G/G_{max})^2 - 1.547(G/G_{max}) + 1]. \quad (23)$$

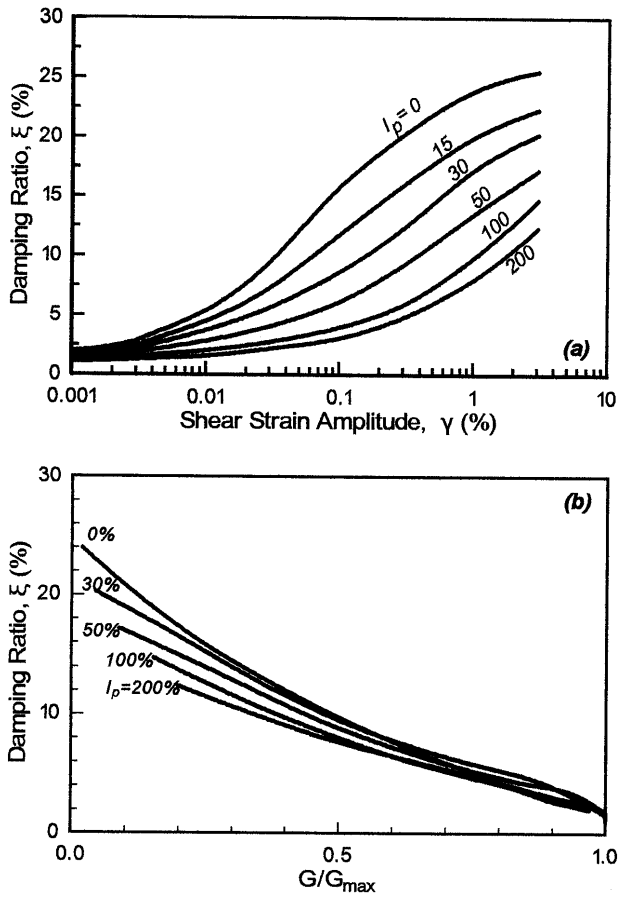

Fig. 8. Experimental curves for the non-linear variation of hysteretic damping ratio proposed by Vucetic and Dobry (1991): (a) $\xi(\%)$-γ relationship; (b) $\xi(\%)$-G/G_{max} relationship

Figure 9 compares Eq. (23) to the experimental curves of Fig. 8(b). The observed differences are relatively small and concern mainly non-plastic soils. Furthermore, the average of the two sets of data may be fitted by the following analytical expression:

$$\xi=0.30g(lp)[1-0.77(G/G_{max})]^2 \tag{24}$$

with

$$g(lp)=0.60+0.40\exp[-0.025(lp)]. \tag{25}$$

The radial variation of damping ratio is computed from Eq. (24), with the modulus ratio expressed in terms of the radial distance (Eq. (18)):

$$\xi=0.30g(lp)[0.23+\{0.77\Lambda(R/r)F(\alpha)\}^{0.72}]^2. \tag{26}$$

Figure 10 shows the radial variation of hysteretic damping ratio resulting from Eq. (26). To focus upon the effects of the loading intensity parameter Λ and the frequency parameter α_i, the damping ratio has been divided by the plasticity dependent factor $g(lp)$. As in the case of the shear modulus ratio, it is observed that, for all combinations of Λ and α_i, the radial variation of damping ratio is most rapid in the immediate vicinity of the pile, within a distance of two to four pile radii. At larger distances, the rate of change is substantially reduced and the damping ratio tends asymptotically to the corresponding free field value $[\xi\rightarrow 0.016g(lp)]$. In addition, the damping ratio at the pile-soil interface $\xi_i=\xi(R)$ is independent of the loading frequency parameter α_i.

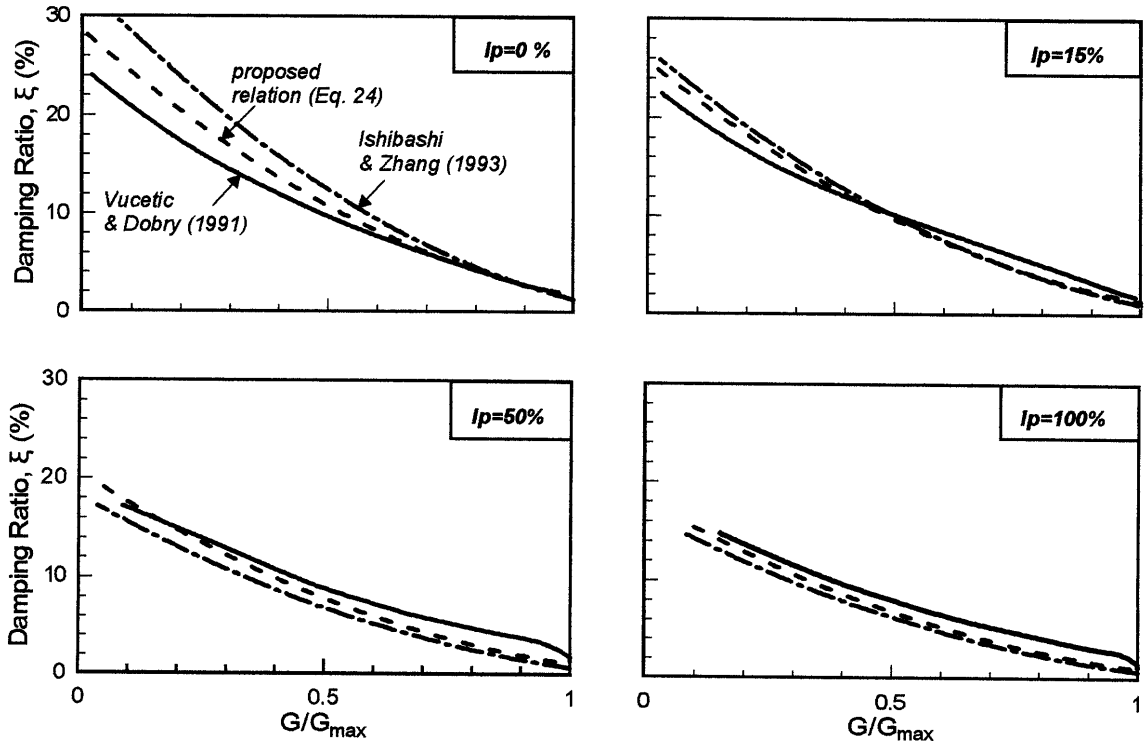

Fig. 9. Comparison of proposed $\xi(\%)$-G/G_{max} relationship to empirical relationships proposed by Vucetic and Dobry (1991) and Ishibashi and Zhang (1993)

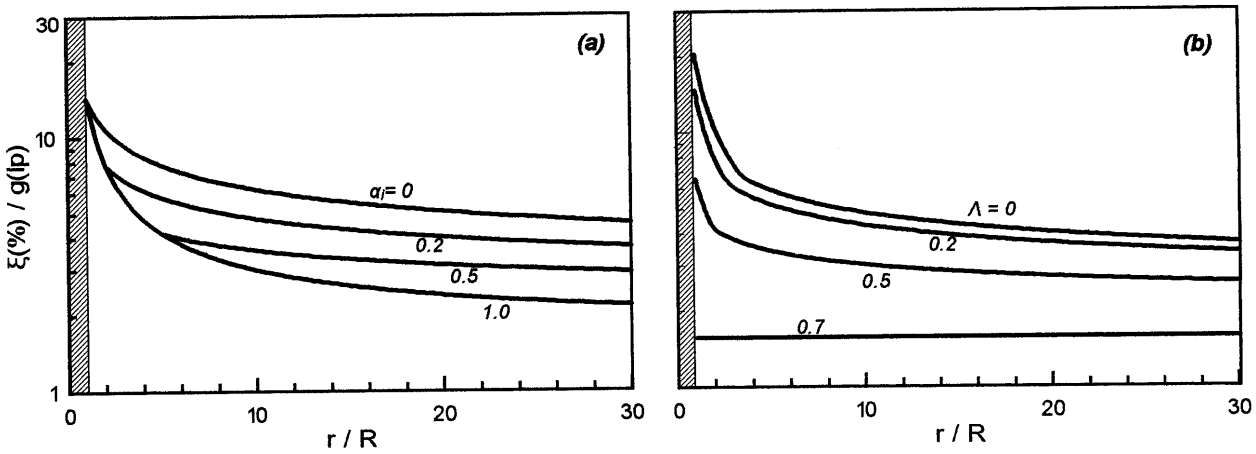

Fig. 10. Radial variation of hysteretic damping ratio: (a) Effect of loading frequency a_i; (b) Effect of loading intensity Λ

NON-LINEAR DYNAMIC SOIL IMPEDANCE

The dynamic soil impedance is derived from solution of a differential equation of motion for a vertically excited inhomogeneous soil layer enclosing a pile element of unit thickness. However, a rigorous solution for this equation is not possible for the variation of soil properties derived previously. Hence, the soil around the pile is divided into a small number of zones, so that simpler relationships can be employed to fit the soil properties in each zone. Here, it was found sufficient to use four zones with inner bounds at radii $r_0=R$, $r_1=2R$, $r_2=6R$ and $r_3=30R$ (Fig. 11). The complex shear modulus of the zones is defined as:

$$G^*(r)=G(r_n)\{1+2i\xi(r_n)\}(r/r_n)^{m_n} \quad (n=0, 1, 2, 3) \quad (27)$$

and

$$m_n=\begin{cases}\log\{G(r_{n+1})/G(r_n)\}/\log(r_{n+1}/r_n) & (n=0, 1, 2)\\ 0.0 & (n=3)\end{cases} \quad (28)$$

while the corresponding hysteretic damping ratio is defined from Eq. (24).

For each zone, the general solution of Eq. (4) is written as (Gazetas and Dobry, 1984; Veletsos and Dotson 1986):

$$W_n(r)=\zeta^{-m_n/2}[A_nH^{(1)}_{\kappa_n-1}(\kappa_n\lambda_n\zeta_n^{1/\kappa_n}) + B_nH^{(2)}_{\kappa_n-1}(\kappa_n\lambda_n\zeta_n^{1/\kappa_n})] \quad (29)$$

where $\zeta_n=r/r_n$, $\kappa_n=2/(2-m_n)$, $H^{(1)}_\kappa$ and $H^{(2)}_\kappa$ are Hankel functions of order κ and first and second kind respectively, $\lambda_n=a_n/(1+2i\xi_n)$, $\alpha_n=\omega r_n/V_n$ and V_n is the shear wave velocity at the inner boundary of each zone. The integration constants A_n, B_n are determined so that stresses and displacements are continuous at the borders of the zones, while displacements become zero at a very large radial distance ($r\to\infty$).

Consequently, the impedance of the soil slice around the pile is determined as:

$$I_z=-2\pi G_i^*(dW/dr)_{r=R} \quad (30)$$

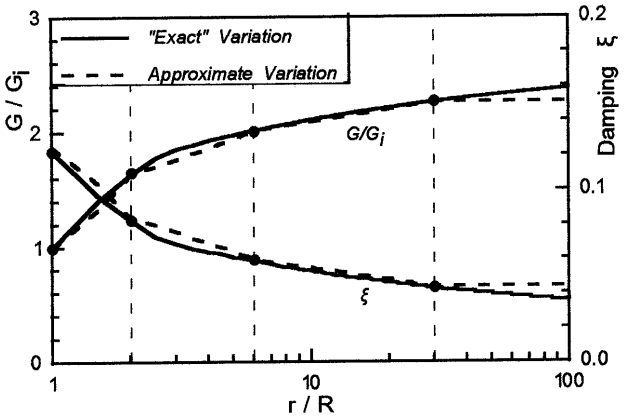

Fig. 11. Example fitting of dynamic soil properties used for the analytical computation of soil impedance (a_i=0.50, Λ=0.50)

or

$$I_z=2\pi G_i^*\lambda_0\{A_0H^{(1)}_{k_0}(\kappa_0\lambda_0)+B_0H^{(2)}_{k_0}(\kappa_0\lambda_0)\} \quad (31)$$

where

$$G_i^*=G_i(1+2i\xi_i). \quad (32)$$

Equation (31) represents a complex function which is commonly written in the simplified form:

$$I_z=K_z+i\omega C_z. \quad (33)$$

The real and imaginary parts of the dynamic soil impedance, K_z and C_z, are shown in Fig. 12 for different values of the loading intensity parameter Λ, the plasticity index lp and the frequency parameter $a_i=\omega R/V_{ff}$, where V_{ff} denotes the shear wave velocity of the free-field. For the sake of a generalised presentation, K_z and C_z are shown in a non-dimensional form, with reference to the pile radius R, the frequency of loading ω, the free-field shear wave velocity V_{ff} and the corresponding shear modulus G_{ff} ($=G_{\max}$). It is observed that soil nonlinearity may reduce drastically the moduli of Winkler springs and dashpots K_z and C_z. In general, the reduction is larger for

(a) high frequency loading, and for

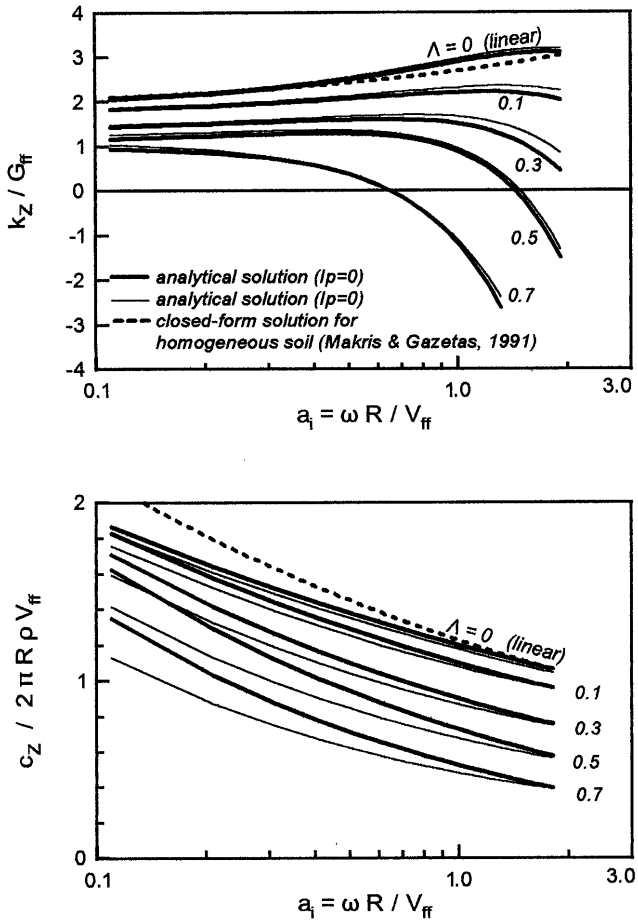

Fig. 12. Analytical solutions for the dynamic impedance parameters K_z and C_z of non-linear soil

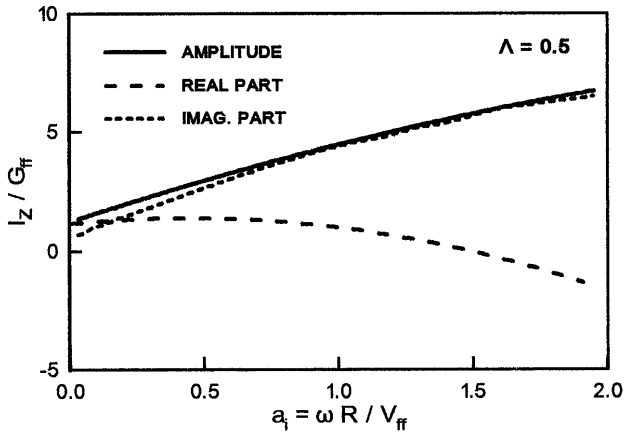

Fig. 13. Relative contribution of the real and the imaginary parts to the amplitude of soil impedance

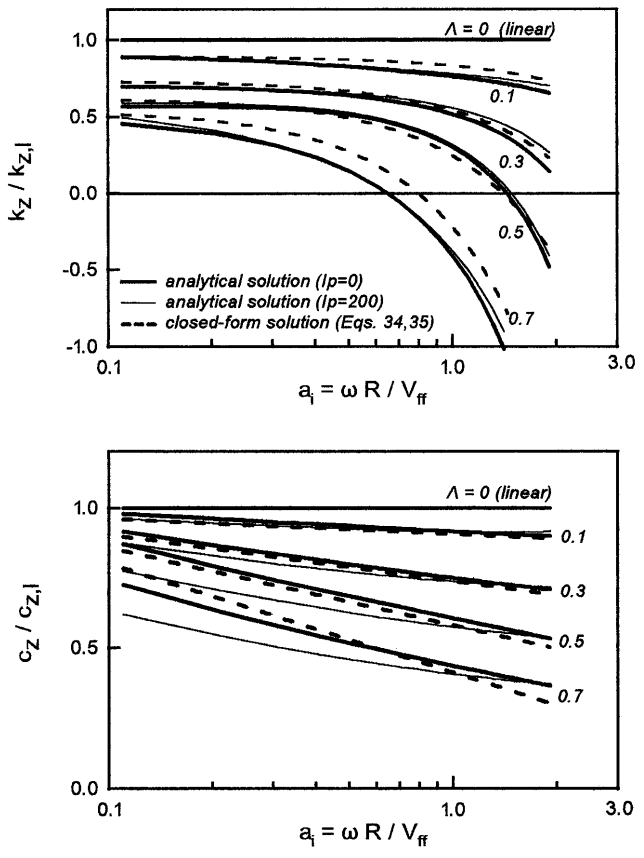

Fig. 14. Comparison between analytical and closed-form approximate relationships for the prediction of the (normalised) dynamic soil impedance parameters K_z and C_z

(b) large values of the parameter Λ, corresponding to more intense dynamic loading but also to less plastic soils which degrade faster with increasing cyclic strain amplitude (e.g. Fig. 5).

The plasticity index lp has a minor direct effect, but affects indirectly the analytical predictions through the loading intensity parameter Λ.

The relative contribution of the real (in-phase) and the imaginary (out of phase) parts of soil impedance is evaluated in Fig. 13 for two specific values of the loading intensity parameter: $\Lambda=0$ (linear) and $\Lambda=0.50$. In both cases, the imaginary part of soil impedance dominates over the real part, except for very low loading frequencies. This observation implies that most of the reaction to the axial oscillation of a pile element comes from the inertia of the surrounding soil rather than from its stiffness. Naturally, this trend is reversed as the frequency of oscillation is reduced and the loading changes gradually from dynamic to quasi-static.

In Fig. 14, the analytical predictions are normalised against the corresponding values for $\Lambda=0$, e.g. the linear elastic solutions for a homogeneous soil with the non-degraded properties of the free-field. In an approximate form, these data may be described by the following closed-form relationships:

$$K_z/K_{z,l}=(1+1.20\Lambda)^{-1}\left[1-\frac{0.60\Lambda}{(1-\Lambda)}a_i^{1.50}\right] \tag{34}$$

$$C_z/C_{z,l}=1-0.84\Lambda(1+0.66\log a_i) \tag{35}$$

$K_{z,l}$ and $C_{z,l}$ denote the impedance parameters for $\Lambda=0$, and may be expressed in closed form as (Makris and Gazetas, 1993):

$$K_{z,l}=1.8G_{ff}(1+0.5\sqrt{a_i}) \tag{36}$$

$$C_{z,I}=(C_{z,I})_{\text{radiation}}+(C_{z,I})_{\text{hysteresis}}$$
$$=2.4a_i^{-1/4}\pi R\rho V_{ff}+2\xi_0 K_{z,I}/\omega \quad (37)$$

where $\xi_0=0.016g(lp)$ denotes the free field value of ξ. Equations (34) and (35) are shown with dotted lines in Fig. 14 in comparison to the relevant analytical solutions, while Eqs. (36) and (37) are compared to the analytical solutions for $\Lambda=0$ in Fig. 12.

The effect of hysteretic damping on the impedance parameters K_z and C_z is evaluated in Fig. 15. Two sets of analytical predictions are compared: one that consistently takes into account the hysteretic damping and another that ignores it. Except for low values of the non-dimensional frequency parameter a_i (<0.20), the difference between the two sets of predictions increases with loading intensity, but remains overall low in proportion to the values of K_z and C_z. This suggests that, as for homogeneous soils, the major mechanism leading to loss of energy in axisymmetric vibration problems is radiation to the free field rather than hysteretic energy dissipation in the soil. For the low values of a_i, material damping appears to be important with regard to the dashpot modulus C_z. However, even in this case, the effect of material damping on the spring modulus K_z and, by extension, on the magnitude of soil impedance I_z is still small.

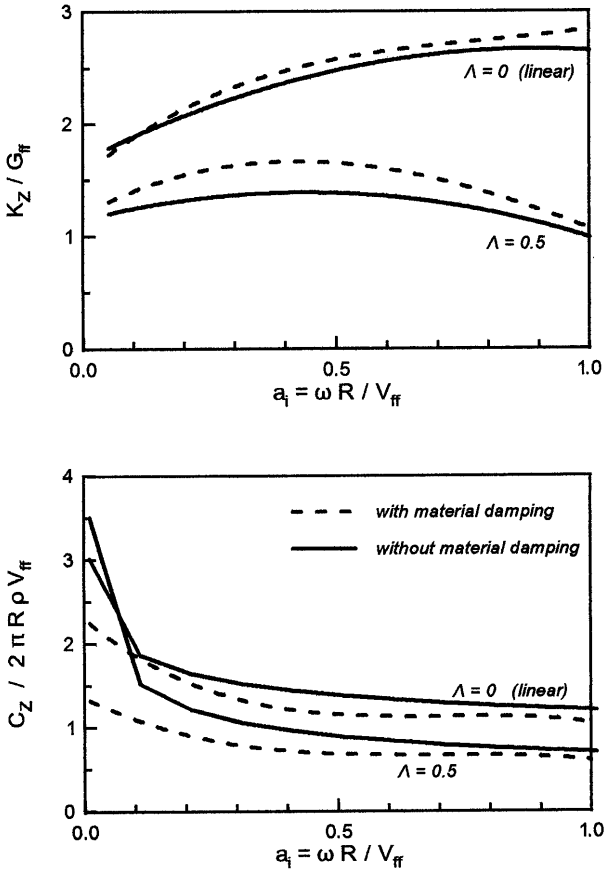

Fig. 15. Effect of material damping on non-linear dynamic soil impedance parameters K_z and C_z

EFFECT OF SLIPPAGE AT THE PILE-SOIL INTERFACE

The previous analysis is based on the assumption that no slippage takes place between the pile and the soil. When this occurs, the equivalent impedance of the soil is drastically reduced, since the displacement of the pile segment and the hysteretic energy loss corresponding to a given dynamic loading amplitude may increase significantly.

Figure 16 shows the elasto-plastic load-displacement relationships corresponding to the spring and slider model which is used here to simulate the cyclic response of the pile-soil interface. Under loading with controlled (constant) static displacement δ_{st} and dynamic displacement amplitude $\pm\delta$, slippage may occur under one of the following two conditions:

(a) The peak external load P_0+P is larger than the yield

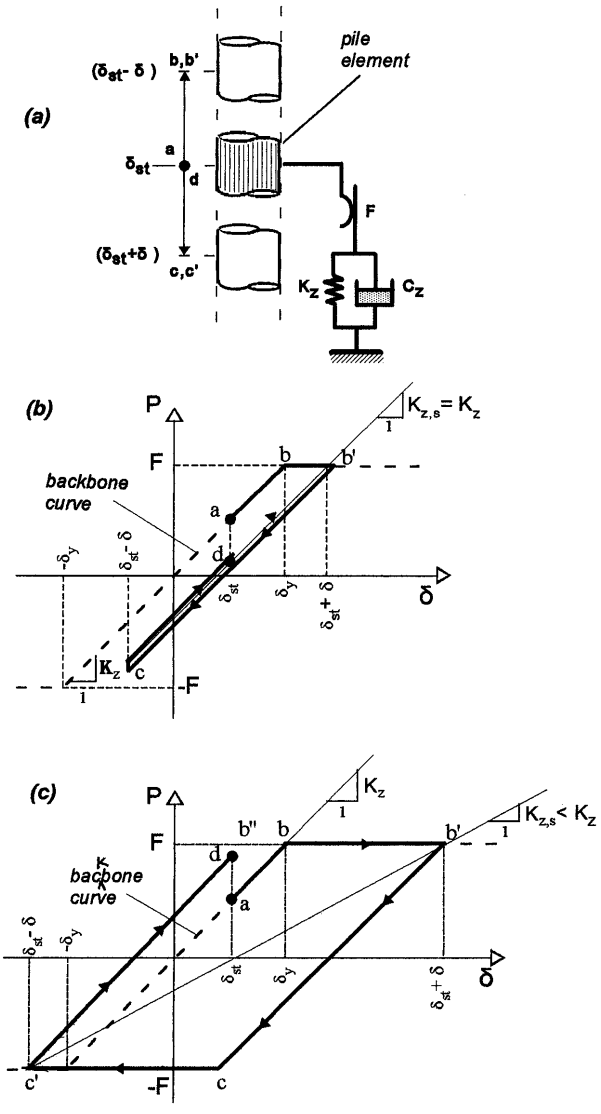

Fig. 16. Simplified simulation of the effects of slippage at the pile-soil interface: (a) Winkler model of pile element; (b) One-way slippage with $P_{st}+P>F$ and $P<F$; (c) Two-way slippage with $P_{st}+P>F$ and $P>F$

load $F=\pi Df$, but the dynamic load amplitude P is lower than F (Fig. 16(b)). In this case, slippage will occur only upon first-time loading, from δ_{st} to $\delta_{st}+\delta$ (branch abb′ of the loop), while subsequent unloadings and reloadings will be sustained by the spring-slider system without further slippage (branch b′cd of the loop). In parallel, the static force applied on the pile segment is reduced from P_{st} to $P_{st}^{*}=F-P$. Thus, neglecting permanent slippage upon first-time loading, the equivalent linear elasto-plastic impedance of the soil I_{zs} is essentially equal to the equivalent linear elastic impedance I_z.

(b) The peak external load $P_{st}+P$, as well as the dynamic load amplitude P are larger than the yield load F (Fig. 16(c)). In this case, the static load is reduced to zero during first-time loading, but this is not enough to avoid slippage at the slider. Hence, slippage will occur during all subsequent loadings and unloadings, whenever the dynamic load reaches the yield limit (branches bb′ and cc′ of the loop). As a result, the equivalent linear elasto-plastic impedance of the soil I_{zs}, represented by the slope of the diagonal b′c′ of the loop in Fig. 16(c), becomes smaller than the elastic one I_z. In addition, the proportion of hysteretic energy loss during cyclic loading will increase as the load-displacement loop widens under constant dynamic displacement amplitude δ.

Figure 17 shows actual load-displacement measurements from recently published experiments of two-way cyclic loading of a marine clay-steel interface (Desai and Rigby, 1997). It may be observed that the model behaviour presented earlier resembles fairly well the experimental results. Furthermore, due to its simple analytical formulation, it allows expression of the relative effects of slippage on the dynamic soil stiffness and damping through closed-form relations.

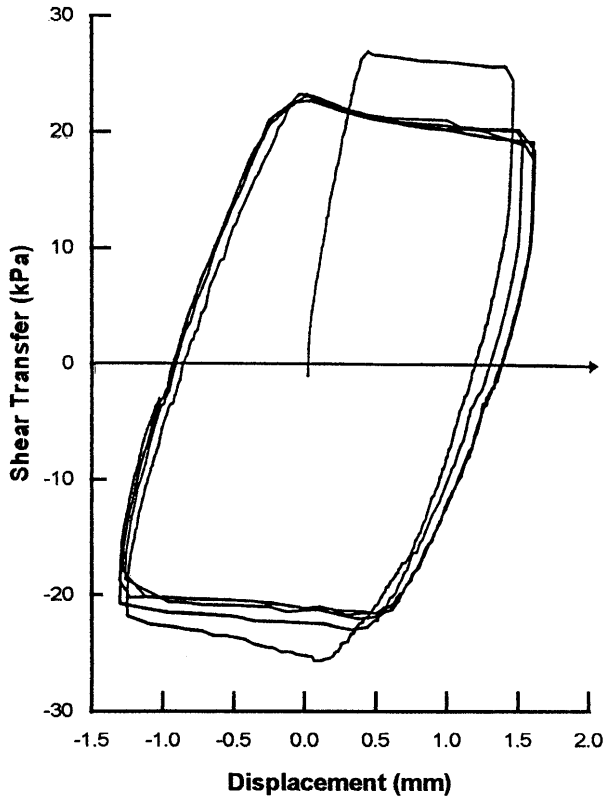

Fig. 17. Results for two-way cyclic loading of a marine clay-steel interface from field tests on an instrumented pile segment (Desai and Rigby, 1997)

Based on the geometry of the load-displacement loop in Fig. 16(c), the relative effect of slippage on dynamic soil impedance may be written as:

$$I_{zs}=I_z(F/P)=I_z(f/\tau_i)\leq I_z \tag{38}$$

where τ_i is the dynamic shear stress that would have developed at the pile-soil interface if slippage had not occurred, and f is the skin friction.

It is important to note here that f depends upon the rate of loading and consequently it is not necessarily the same with the skin friction under static loading. This is especially true for clayey soils, which generally have a more pronounced viscous behaviour, where reported experimental values for dynamic loading exceed static values by 50% or more (Bea and Audibert, 1979; Kraft et al., 1981; Bergdahl and Hult, 1981). The same data suggest that, in the absence of site specific test results, f should be increased relative to its static value by about 10–15% for each ten-fold increase in the rate of loading.

To account for the hysteretic energy loss due to slippage at the pile soil interface, an equivalent damping ratio ξ_s is obtained that must be added to the hysteretic damping ratio of the soil ξ. Based on the area of a complete loop ΔE_s and the equivalent elastic energy $E_s=(1/2)F\delta$, ξ_s is written as follows:

$$\xi_s=(1/4\pi)\Delta E_s/E_s=(2/\pi)(1-f/\tau_i). \tag{39}$$

The dynamic impedance parameters K_{zs} and C_{zs} of the equivalent linear Winkler springs and dashpots, may be subsequently derived from combination of Eqs. (38) and (39) as follows:

$$K_{zs}=\begin{cases}K_z & \tau_i\leq f\\ K_z(f/\tau_i) & \tau_i\geq f\end{cases} \tag{41}$$

and

$$C_{zs}=\begin{cases}C_z & \tau_i\leq f\\ C_z(f/\tau_i)+2\xi_s K_{zs}/\omega & \tau_i\geq f.\end{cases} \tag{42}$$

The resulting variation of elasto-plastic impedance parameters K_{zs} and C_{zs} are plotted in Fig. 18 as functions of the cyclic shear stress ratio τ_i/f, for two extreme values of the dimensionless frequency parameter: $a_i=0.1$, corresponding to quasi-static cyclic loading, and $a_i=1.0$, corresponding to high frequency dynamic loading. It may be observed that the effect of slippage on each impedance parameter is different. Namely, K_{zs} is systematically lower than K_z regardless of loading frequency, while C_{zs} is practically the same as C_z for quasi-static cyclic loading and systematically lower than C_z for high frequency dynamic loading.

According to Eq. (41), these differences can be attri-

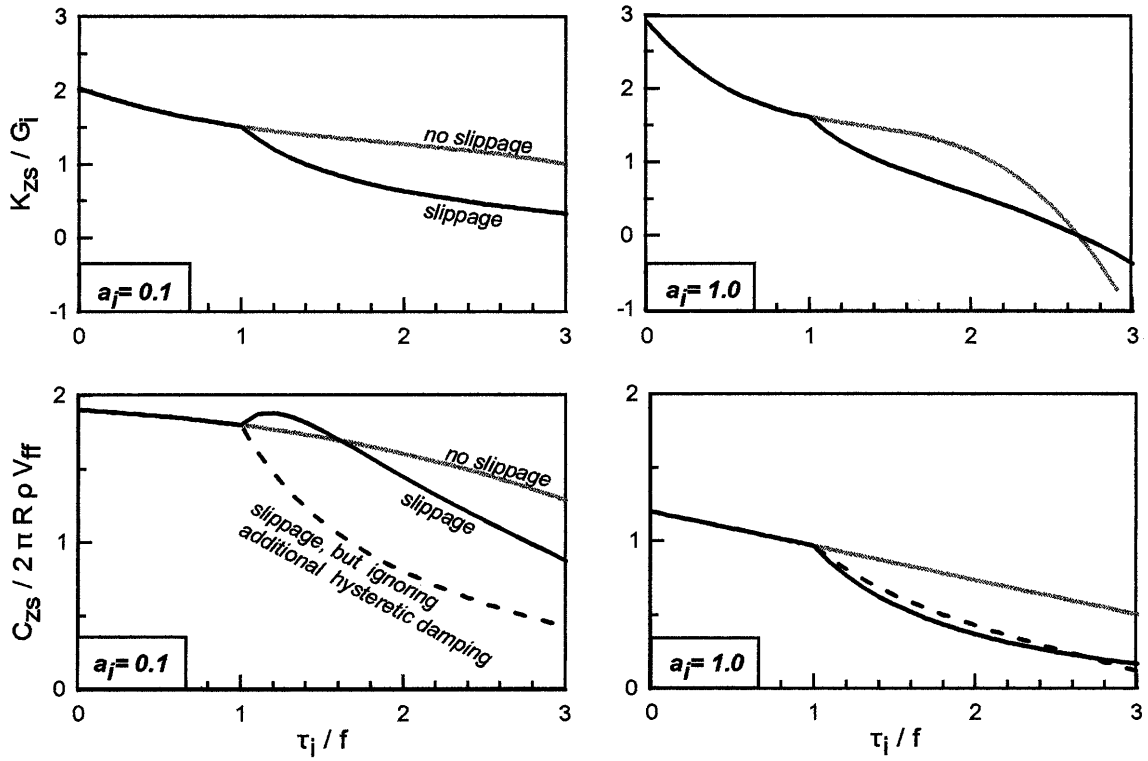

Fig. 18. Effect of slippage at the pile-soil interface on the dynamic impedance parameters K_z and C_z

buted to two counteracting mechanisms which control the dashpot parameter C_{zs}:

(a) the hysteretic energy loss **at the pile-soil interface**, which is inversely proportional to frequency ω, and

(b) the reduction of radiation and hysteretic damping **in the soil**, in proportion to the shear stress ratio f/τ_i, which is nearly independent from frequency ω.

At low frequencies mechanism (a) is relatively more significant and may overshadow mechanism (b), while at higher frequencies this mechanism is gradually reversed.

To support this interpretation, the dashed lines in Fig. 18 represent the computed values of C_{zs} when the additional hysteretic damping due to slippage is not taken into account. In that case, the effect of slippage is solely dominated by the aforementiond mechanism (b), and consequently the elasto-plastic dashpot parameter is systematically reduced at low, as well as at high frequencies.

CONCLUSION

Analytical solutions are provided for the radial variation of soil properties and the corresponding dynamic soil impedance based on experimental data for the non-linear soil response and the slippage at the pile soil interface. In addition, the effects of these mechanisms are evaluated with the aid of parametric analyses for different loading characteristics, pile geometries and soil properties. The main general conclusions derived from these analyses are the following:

(a) **Dynamic shear stress amplitudes** induced to the soil decrease with radial distance away from the pile. The rate of decrease becomes slower with increasing frequency of vibration and is practically independent of the initial (at rest) radial distribution of soil properties.

(b) Due to non-linear soil response, the **dynamic shear modulus** of the soil increases, and the **hysteretic damping** ratio decreases with radial distance. These changes are rapid within a distance of 2–4 pile radii, and become more pronounced as the intensity and the frequency of dynamic loading increase, while the soil becomes less plastic.

(c) Soil nonlinearity reduces significantly the **dynamic soil impedance**, expressed by the moduli of the equivalent-linear Winkler springs and dashpots, relative to the values for a linear soil with the non-degraded properties of the free-field. As with soil properties, the degradation of soil impedance becomes more pronounced as the intensity and the frequency of dynamic loading increase, and the soil becomes less plastic.

(d) **Slippage** at the pile-soil interface may reduce further the soil impedance, mainly in the case of two-way cyclic loading (compression-extension) with reversing slip. For the equivalent linear Winkler springs, this effect is systematic and practically independent of loading frequency. On the other hand, for the corresponding dashpots, slippage becomes practically important at relatively high frequencies of loading only.

(e) The analytical predictions of non-linear dynamic soil impedance may be expressed with reasonable accuracy by relatively simple, **closed-form relationships.**

APPENDIX I: DYNAMIC AXIAL RESPONSE OF PILES SUPPORTED BY NON-LINEAR (WINKLER) SPRINGS AND DASHPOTS

The dynamic moduli of the Winkler springs and dashpots derived in the article may be consequently used to compute the dynamic axial response of single piles embedded in non-linear soil. The procedure which has to be followed for this purpose is basically the same as for piles in linear soil, and may be briefly outlined with the aid of Fig. I.1. For harmonic steady-state oscillation of the pile, expressed in the form:

$$\Delta(z, t)=\delta(z)e^{i\omega t} \tag{I.1}$$

dynamic equilibrium of a pile element requires that:

$$ES\frac{d^2\delta(z)}{dz^2}-(K_{zs}+i\omega C_{zs}-m\omega^2)\delta(z)=0 \tag{I.2}$$

where z denotes the depth from the ground surface, E and S denote the Young's modulus and the cross-sectional area of the pile while m is the mass of the pile per unit length.

The general solution of this equation is written as (e.g. Makris and Gazetas, 1993):

$$\delta=A_1e^{Qz(\cos\theta+i\sin\theta)}+A_2e^{-Qz(\cos\theta+i\sin\theta)} \tag{I.3}$$

where

$$Q=\left[\frac{(K_{zs}-m\omega^2)^2+(\omega C_{zs})^2}{(ES)^2}\right]^{1/4} \tag{I.4}$$

and

$$\tan(2\theta)=\frac{\omega C_{zs}}{K_{zs}-m\omega^2}. \tag{I.5}$$

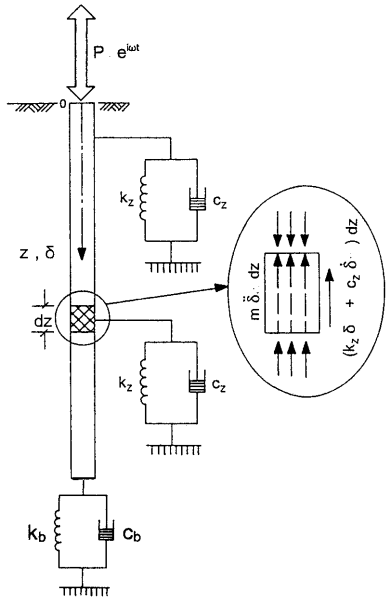

Fig. 19. Winkler model for a vertically vibrating pile (based on Makris and Gazetas, 1993)

For a given load or displacement amplitude applied to the pile head, the integration constants A_1 and A_2 are computed by enforcing the continuity of stresses and displacements along the pile axis and assuming appropriate values for the spring and dashpot moduli supporting the pile tip (K_b, C_b in Fig. I.1).

As a result of soil nonlinearity, Eq. (I.3) is an implicit relation since δ is expressed as a function of K_{zs} and C_{zs} which, in turn, depend upon δ. Hence, an iterative solution has to be followed in order to obtain the pile response. Details on this procedure are provided by Michaelides et al. (1997).

LIST OF MAIN SYMBOLS

II.1 Latin Symbols

- a non-dimensional frequency parameter, defined in terms of the free-field shear wave velocity and the radial distance ($a=\omega r/V_{ff}$)
- a_i the value of a corresponding to the pile-soil interface ($a_i=\omega R/V_{ff}$)
- C_z frequency dependent modulus of equivalent Winkler dashpot
- C_{zs} frequency dependent modulus of equivalent Winkler dashpot with effect of slippage
- D diameter of pile element ($=2R$)
- f unit skin friction
- F yield load of the pile-soil interface
- g damping factor depending on soil plasticity
- $G_{\max}$ shear modulus of soil for very small shear strain amplitude ($\gamma<10^{-5}$)
- G shear modulus of soil at radial distance r from the pile axis
- G_{ff} free field (elastic) shear modulus of soil ($G_{ff}=G_{\max}$)
- G_i shear modulus of soil at the pile-soil interface ($r=R$)
- G^* complex shear modulus of soil at radial distance r from the pile axis
- G_{ff}^* complex shear modulus of soil at the free field
- G_i^* complex shear modulus of soil at the pile-soil interface ($r=R$)
- H Hankel functions
- I_z composite (complex) dynamic soil impedance
- I_{zs} composite (complex) dynamic soil impedance with effect of slippage
- J Bessel function of first kind
- K_z frequency dependent modulus of equivalent Winkler spring
- K_{zs} frequency dependent modulus of equivalent Winkler spring with effect of slippage
- P_{st} static axial load of pile element
- P dynamic axial load amplitude of pile element
- r radial distance from pile axis
- R pile radius
- V shear wave velocity of soil at radial distance r from the pile axis
- V_{ff} free field (elastic) shear wave velocity of soil
- V_i shear wave velocity of soil at the pile-soil interface ($r=R$)
- Y Bessel function of second kind

II.2 Greek Symbols

- α ($=\omega r/V_i$) nondimensional frequency parameter, defined in terms of the shear wave velocity at the pile-soil interface and the radial distance
- α_i ($=\omega R/V_i$) the value of α at the pile-soil interface
- δ_{st} static axial displacement of pile element
- δ dynamic axial displacement amplitude of pile element
- δ_y yield displacement at the pile-soil interface
- ξ hysteretic damping ratio
- ξ_{ff} free field hysteretic damping ratio [$\xi_{ff}=0.016g(lp)$]
- ξ_i hysteretic damping ratio at the pile-soil interface ($r=R$)
- τ_{st} static shear stress at radial distance r from the pile axis
- τ dynamic shear stress amplitude at radial distance r from the pile

axis
ω circular frequency

REFERENCES

1) Andersen, K. H., Kleven, A. and Heien, D. (1988): "Cyclic soil data for design of gravity structures," ASCE, J. of Geotech. Engrg. Division, Vol. 114, No. 5, pp. 517–539.
2) Baguelin, F. and Frank, R. (1979): "Theoretical studies of piles using the finite-element method," Numerical Methods in Offshore Piling, London: ICE, pp. 83–91.
3) Bea, R. G. and Audibert, J. M. E. (1979): "Behaviour of dynamically loaded pile foundations," Proc. BOSS'79, pp. 728–745.
4) Bergahl, U. and Hult, G. (1981): "Load tests on friction piles in clay," Proc. 10th Int. Conf. on SMFE, Stockholm, pp. 625–630.
5) Desai, C. S. and Rigby, C. B. (1997): "Cyclic interface and joint shear device including pore pressure effects," J. of Geotech. and Geoenvironmental Engrg., ASCE, Vol. 123, No. 6, pp. 568–579.
6) Dotson, K. W. and Veletsos, A. S. (1990): "Vertical and torsional impedances for radially inhomogeneous viscoelastic soil layers," Soil Dynamics and Earthquake Engrg., Vol. 9, No. 3, pp. 110–119.
7) Gazetas, G. (1982): "Shear vibration of vertically inhomogeneous earth dams," Int. J. for Numerical and Analytical Methods in Geomechanics, Vol. 6, No. 1, pp. 219–241.
8) Gazetas, G. and Dobry, R. (1984): "Simple radiation damping model for piles and footings," J. of Engrg. Mechanics, ASCE, Vol. 110, No. 6, pp. 937–956.
9) Ishibashi, I. and Zhang, X. (1993): "Unified dynamic shear moduli and damping ratios of sand and clay," Soils and Foundations, Vol. 33, No. 1, pp. 182–191.
10) Iwasaki, T., Tatsuoka, F. and Takagi, Y. (1978): "Shear moduli of sands under cyclic torsional shear loading," Soils and Foundations, Vol. 18, No. 1, pp. 39–56.
11) Ishihara, K. (1982): "Evaluation of soil properties for use in earthquake response analysis," Num. Mod. Geom., Dungar, R., Pande, G. N. and Studer, J. A. (eds.), pp. 237–259.
12) Kraft, L. M., Cox, W. R. and Verner, E. A. (1981): "Pile load tests: Cyclic loads and varying load rates," J. of Geotech. Engrg. Division, ASCE, Vol. 107, No. 1, pp. 1–19.
13) Makris, N. and Gazetas, G. (1993): "Displacement phase differences in a harmonically oscillating pile," Géotechnique, Vol. 43, No. 1, pp. 135–150.
14) Masing, G. (1926): "Eigenspannumyen und verfeshungung beim messing," Proc. Inter. Congress for Applied Mechanics, pp. 332–335.
15) Michaelides, O., Gazetas, G., Bouckovalas, G. and Chrysikou, E. (1997): "Approximate nonlinear dynamic axial response of piles," Geotechnique, accepted for publication.
16) Morse, P. M. and Ingard, K. U. (1968): Theoretical Acoustics, McGraw-Hill Book Co., New York, N.Y.
17) Novak, M. (1974): "Dynamic stiffness and damping of piles," Can. Geotech. J., Vol. 11, No. 4, pp. 574–598.
18) Novak, M. (1977): "Vertical vibration of floating piles," J. of Engrg. Mechs. Division, ASCE, Vol. 103, No. EM1, pp. 153–168.
19) Novak, M. and Sheta, M. (1980): "Approximate approach to contact effects of piles," Special Technical Publication on Dynamic Response of Pile Foundations: Analytical Aspects, ASCE, O'Neill, M. W. and Dobry, R. (eds.).
20) Randolph, M. F. and Wroth, P. C. (1978): "Analysis of deformation of vertically loaded piles," J. of the Geotech. Engrg. Division, ASCE, Vol. 104, No. GT12, pp. 1465–1488.
21) Sagaseta, C., Cuellar, V. and Pastor, M. (1991): "Modelling stress-strain-time behaviour of natural soils: Cyclic loading," 10th European Conf. on SMFE, Firenze, Italy, Vol. III, pp. 981–1002.
22) Seed, H. B. and Idriss, I. M. (1970): "Soil moduli and damping factors for dynamic response analysis," Report No. EERC 75-29, Earthquake Engrg. Research Center, Univ. of California, Berkeley.
23) Veletsos, A. S. and Dotson, K. W. (1986): "Impedances of soil layer with disturbed boundary zone," J. of the Geotech. Engrg. Division, ASCE, Vol. 112, No. 3, pp. 363–368.
24) Veletsos, A. S. and Dotson, K. W. (1988): "Vertical and torsional vibration of foundations in inhomogeneous media," J. of the Geotech. Engrg. Division, ASCE, Vol. 114, No. 9, pp. 1002–1021.
25) Vucetic, M. and Dobry, R. (1990): "Effect of soil plasticity on cyclic response," J. of Geotech. Eng., ASCE, Vol. 117, No. 1, pp. 89–107.